c-di-AMP, a likely master regulator of bacterial K+ homeostasis machinery, activates a K+ exporter. Cereija TB, Guerra JPL, Jorge JMP, Morais-Cabral JH. Proc Natl Acad Sci U S A. 2021 Apr 6;118(14):e2020653118. doi: 10.1073/pnas.2020653118.

c-di-AMP, a likely master regulator of bacterial K^+ homeostasis machinery, activates a K^+ exporter

Tatiana B. Cereija[a,b], João P.L. Guerra[a,b,1], João M.P. Jorge [a,b], João H. Morais-Cabral[a,b,2]

[a] IBMC – Instituto de Biologia Molecular e Celular, Universidade do Porto, Portugal

[b] i3S – Instituto de Investigação e Inovação em Saúde, Universidade do Porto, Portugal

[1] Current address: UCIBIO-Requimte, Departamento de Química, Faculdade de Ciências e Tecnologia, Universidade Nova de Lisboa, Portugal

[2]Corresponding author

Correspondence should be addressed to: João H. Morais-Cabral (i3S, Rua Alfredo Allen, 208, 4200-135 Porto, Portugal; Tel. +351 226 074 900; E-mail: jcabral@ibmc.up.pt)

Classification

Research report – Direct submission

Keywords

KhtT, KhtU, KhtTU, *B. subtilis*, RCK domain, K^+/H^+ antiporter.

Abstract

c-di-AMP is a second messenger with roles in virulence, cell wall and biofilm formation and surveillance of DNA integrity in many bacterial species, including pathogens. Strikingly, it has also been proposed to coordinate the activity of the components of K^+ homeostasis machinery, inhibiting K^+ import and activating K^+ export. However, there is a lack of quantitative evidence supporting the direct functional impact of c-di-AMP on K^+ transporters. To gain a detailed understanding of the role of c-di-AMP on the activity of a component of the K^+ homeostasis machinery in *B. subtilis*, we have characterized the impact of c-di-AMP on the functional, biochemical and physiological properties of KhtTU, a K^+/H^+ antiporter composed by the membrane protein KhtU and the cytosolic protein KhtT. We have confirmed c-di-AMP binding to KhtT and determined the crystal structure of this complex. We have characterized *in vitro* the functional properties of KhtTU and KhtU alone and quantified the impact of c-di-AMP and of pH on their activity, demonstrating that c-di-AMP activates KhtTU and that pH increases its sensitivity to this nucleotide. Based on our functional and structural data we were able to propose a mechanism for the activation of KhtTU by c-di-AMP. In addition, we have analyzed the impact of KhtTU in its native bacterium, providing a physiological context for the regulatory function of c-di-AMP and pH. Overall, we provide unique information that supports the proposal that c-di-AMP is a master regulator of K^+ homeostasis machinery.

Significance statement

The importance of di-nucleotides in the control of bacterial physiology is still being uncovered. One of these molecules is c-di-AMP, thought to control the mechanisms of import and export of potassium ions in many bacteria, including pathogens. Maintaining a balanced internal concentration of potassium is crucial for bacterial viability, even during infection. However, there has been a lack of data showing that c-di-AMP effectively changes the activity of potassium transporters. Here, we demonstrate that c-di-AMP increases the activity levels of a potassium exporter and that pH increases the sensitivity of the transporter to c-di-AMP. Our quantitative data supports therefore, the central role of c-di-AMP in the control of the potassium homeostasis machinery in bacteria.

Introduction

bis-(3´,5´)-cyclic diadenosine monophosphate (c-di-AMP) is part of an expanding family of cyclic dinucleotides, which includes c-di-GMP and cGAMP, that function as important bacterial signaling molecules and are sensed by the innate immune response during infection (1-3). c-di-AMP is present in many bacteria, including *Bacillus subtilis* and pathogens such as *B. anthracis, S. aureus , S. pneumoniae, S. pyogenes* and *L. monocytogenes* (4-8). In contrast, *E. coli* lacks the enzymes that synthesize c-di-AMP. This dinucleotide has roles in central metabolism (9), cell wall (10, 11) and biofilm formation (12, 13), DNA integrity (14) and virulence (15). c-di-AMP has also been proposed as a master regulator of the K^+ homeostasis machinery (16-19). In bacteria and archaea, high intracellular K^+ is not just crucial for the activity and stability of the ribosome and setting the membrane electrical potential (20, 21), it also has roles in pH homeostasis, determining internal pressure and in the adaptation to extracellular osmotic changes (22-24). For example, upon hyper-osmotic challenge the intracellular concentration of K^+ in *B. subtilis* will rise from 300 mM to 600-700 mM, during the first phase of the adaptation mechanism, decreasing back to 300 mM in the second phase (25). It is therefore crucial that the activity of dedicated K^+ importers and exporters is tightly controlled.

The proposal that c-di-AMP has a central role in the regulation of the K^+ homeostasis machinery in many bacteria, inactivating K^+ import and activating K^+ export (8), has resulted from a series of experimental observations. The nucleotide concentration increases in parallel with intracellular K^+ (17, 26) and elevated c-di-AMP results in osmosensitivity (27, 28). Phenotypical changes are observed when some K^+ transporters are co-expressed in *E. coli* mutant strains with diadenylate cyclases, which catalyze synthesis of c-di-AMP, suggesting that c-di-AMP affects the function of the transporter (29, 30). In addition, c-di-AMP binds to a riboswitch, regulating the transcription levels of some K^+ transport proteins (31) and to regulatory domains or proteins of known and putative K^+ transporters (29, 30, 32-36). However, there is little or no quantitative evidence demonstrating and characterizing a direct functional impact of c-di-AMP on the activity of K^+ transporters and it is not known how c-di-AMP modulation is coordinated with other signaling cues.

To understand the regulatory impact of c-di-AMP on a K^+ transporter protein, we analyzed the mechanism of regulation of the KhtTU K^+/H^+ antiporter from *B. subtilis*. This protein complex is composed by KhtU, a membrane protein that belongs to the CPA2 superfamily of cation/H^+ antiporters, and KhtT, a cytoplasmic protein that is proposed to bind c-di-AMP at its C-terminal RCK_C domain (30, 32-35, 37-40). The genes of the two proteins are organized in an operon that

also includes KhtS, which is thought to associate with KhtU but has unknown function and is absent from many other bacterial species with KhtTU orthologs (37). Using an *E. coli* phenotype complementation assay it was suggested that KhtU alone is active and involved in the export of K^+, while the complex KhtTU is inactive (37). Using an *in vitro* fluorescence-based transport assay with inside-out (everted) vesicles it was demonstrated that KhtTU transports H^+ in response to the external addition of K^+, consistent with K^+/H^+ antiport activity, and that KhtTU is selective for K^+ over Na^+ (38). In addition, it was shown that KhtTU activity is pH dependent, with no activity at pH 7.5 and maximum activity at pH 9.0.

Here, we have performed a structural, biochemical and functional characterization of KhtT, KhtU and of their complex KhtTU and demonstrate that c-di-AMP directly activates KhtTU in a concentration-dependent manner by binding to KhtT and that pH modulates nucleotide activation. Overall, our results strongly support the model where c-di-AMP controls the activity of K^+ transporters in many bacterial species.

Results

Structure of KhtT in complex with c-di-AMP

It has been proposed using a ligand overlay assay that the cytosolic protein of the KhtTU complex, KhtT, binds c-di-AMP (30). We performed isothermal titration calorimetry (ITC) experiments at pH 8.0 with c-di-AMP and KhtT and determined that the dissociation constant is ~130 nM with a stoichiometry of ~0.5, corresponding to 1 c-di-AMP bound per KhtT dimer (Fig. 1 and Table 1). In contrast, similar titrations with c-di-GMP did not show any heat changes at two temperatures (25ºC and 15°C). These results demonstrate that KhtT binds c-di-AMP tightly and specifically.

To gain insights into the interaction between KhtT and its ligand we determined the crystal structure of KhtT:c-di-AMP complex at 1.85 Å (Fig. 2A and SI Appendix, Table S1). The structure reveals a dimer organized in two domains. The C-terminal domain (C-domain) stretches from residue 77 to the C terminus, adopts the typical fold of C-domains of RCK proteins (also known as RCK_C domains) and binds c-di-AMP in the dimer interface. The N-terminal domain (N-domain) runs from the N terminus to residue 67 and has an unusual fold, comprised by a twisted five-antiparallel β-sheet followed by an α-helix. Unlike the C-domain, it appears that the dimeric arrangement of the N-domain is an integral part of its fold since the buried surface area in the N-domain dimer is extensive (~1360 Å^2), while in the C-domain only ~390 Å^2 are buried in the dimer interface. The N- and C- domains are connected by a nine amino acid linker.

We also solved the KhtT:c-di-AMP structure from a different crystal, with diffraction to 3.14 Å (Fig. 2B and SI Appendix, Table S1). This structure shows the same dimeric arrangement but the N- and C-domains have an altered relative position. Superposition of the N-domains of the two structures shows little alterations in that domain and reveal that the C-domain dimer undergoes a rigid-body torsion with extension of the linker region and conversion of its first β-strand into an α-helix (SI Appendix, Fig. S1), demonstrating an impressive flexibility in the arrangement between the N- and C-domains of KhtT.

In both crystal forms, c-di-AMP binds at the interface between the C-domains, adopting a "U"-shaped conformation (Fig. 2C). Its position is stabilized by contacts between the adenine groups and apolar residues (Leu104, Val109, Val117, Gly132 and Ala133), as well as hydrogen bonds with Pro131 and Val117, in each subunit. At the mouth of the binding site, the two Asp108 residues and one Gln111 (from chain B) contact the ribose groups, while the other Gln111 is recruited into the coordination of a calcium ion mediating a crystal contact (SI Appendix, Fig. S2). Strikingly, Arg110 from chain B stretches into the inner part of the "U"-shaped c-di-AMP and contacts the two phosphate groups in c-

di-AMP, one of them directly and the other through bridging by a water molecule that is positioned across the cyclic-phosphate group. A second water molecule also bridges the phosphate and Ala133 from molecule B. This disposition is observed in 3 out of 4 dimers present in the asymmetric unit of the high-resolution structure. In the fourth dimer, the side-chains of Arg110 from both subunits point into the inner part of the c-di-AMP "U" but one of the arginine side chains displays partial occupancy, showing also density for an alternate conformation away from the nucleotide (SI Appendix, Fig. S3). In the low-resolution structure, the c-di-AMP molecule adopts the same disposition in the dimer interface but it is harder to define the details of the binding sites in the two dimers present in the asymmetric unit. Only one of the four Arg110 could be modeled and it displays a similar position to those found in the high-resolution structure.

The contacts established by Arg110 with the c-di-AMP phosphate, the adoption of a very similar disposition by an arginine in the binding site of the RCK_C domain of KtrA from *S. aureus* (34) and its conservation in other KhtT proteins (SI Appendix, Fig. S4) together with thermal shift and ITC analysis of the $KhtT_{R110A}$ mutant (SI Appendix, Fig. S5A-C), establish that the arginine has a crucial role in the binding of the nucleotide.

KhtTU from *B. subtilis* is activated by c-di-AMP

We tested the functional impact of c-di-AMP on KhtTU activity using a previously described fluorescence-based flux assay with everted vesicles (38). Everted vesicles or inside-out vesicles are formed during lysis of bacterial cell membranes, according to a well-established protocol (41) and present the cytoplasmic face of the cell membrane towards the bath solution. We generated KhtTU-vesicles from the *E. coli* strain KNabc (which lacks NhaA, NhaB and ChaA cation/H^+ antiporters) expressing the KhtTU complex. In the assay (Fig. 3A), lactate is first added to the bath solution to promote accumulation of H^+ in the vesicle lumen and generate a H^+ gradient, quenching the fluorescence of ACMA (a H^+-gradient sensitive dye). Efflux of H^+ is initiated by adding K^+ to the bath solution, causing an increase in fluorescence (dequenching), consistent with H^+ efflux coupled to K^+ uptake mediated by KhtTU.

We performed the assay in the presence of signaling nucleotides (added prior to H^+ charging) and saw no change in the dequenching curve with pApA, c-di-GMP, ppGpp or pppGpp relative to no nucleotide addition. However, with c-di-AMP we observed an increase in fluorescence dequenching, strongly indicating that this nucleotide activates KhtTU (Fig. 3A). In contrast, no changes in dequenching were observed with everted vesicles prepared from cells transformed with empty

plasmid (SI Appendix, Fig. S6). To confirm that activation by c-di-AMP resulted from binding to the site shown in the KhtT crystal structure, we replaced the binding site Arg110 for an alanine, produced $KhtT_{R110A}U$-vesicles and measured activity. As expected, this mutant could not be activated by c-di-AMP (Fig. 3B).

Quantification of c-di-AMP activation was done with KhtTU-vesicles titrated at pH 7.5, 8.0 and 8.5 with 50 mM KCl. At all pH values, c-di-AMP was shown to promote the activation of KhtTU in a concentration-dependent manner (Fig. 3C-E). The rate of dequenching at different concentrations of c-di-AMP was determined by fitting a single-exponential to the experimental curves (SI Appendix, Fig. S7). Rate constants were plotted as a function of c-di-AMP concentration and a Hill equation was fitted to these data (Fig. 3F). At pH 7.5, the $K_{1/2}$ of activation by c-di-AMP was ~40 µM with a Hill coefficient of ~1. Lower concentrations of c-di-AMP were required to activate KhtTU at higher pH, with $K_{1/2}$ = 3.6 ± 0.5 µM (Hill coefficient = ~2) at pH 8.0 and $K_{1/2}$ = 0.70 ± 0.08 µM (Hill coefficient = ~2) at pH 8.5. Importantly, the 10-fold increase in c-di-AMP sensitivity of KhtTU between pH 7.5 and pH 8.0 is not explained by an increase in the binding affinity of nucleotide for KhtT. Calorimetry titrations of c-di-AMP into KhtT at pH 7.5 showed a K_D ~40 nM relative to K_D ~130 nM at pH 8.0 (Table 1 and SI Appendix, Fig. S8). This 3-fold change in K_D is well below the 10-fold change necessary to indicate a molecularly significant alteration in the ligand binding energy but if meaningful, it would suggest a decrease in binding affinity at higher pH. The lower constants of dissociation for c-di-AMP binding to KhtT alone relative to the $K_{1/2}$ of activation in the KhtTU complex are expected. The energy required for activation of KhtTU is imparted by the chemical energy released from the interactions established by the nucleotide in its binding site, resulting in higher half concentrations of nucleotide for complex activation than for binding to the regulatory protein alone.

In addition, both basal and maximal activities also increased with higher pH. Basal rates (without c-di-AMP) were ~0.002 s^{-1} at pH 7.5, ~0.003 s^{-1} at pH 8.0 and ~0.004 s^{-1} at pH 8.5, and the maximal rates (with saturating concentrations of c-di-AMP) were ~0.009 s^{-1} and ~0.01 s^{-1} at pH 8.0 and pH 8.5, respectively. We estimated that the maximal rate at pH 7.5 is ~0.007 s^{-1} (see section below).

Importantly, these results demonstrate that KhtTU is activated by both c-di-AMP and pH, becoming more active and more sensitive to c-di-AMP at higher pH.

Mechanisms of activation by c-di-AMP and pH

We gained clues about the underlying mechanism of activation of the KhtTU complex by both c-di-AMP and pH while setting-up the everted vesicle assay. We noticed that the flux properties of vesicles prepared at pH 8.0 differed from those prepared at pH 7.0. In particular, when tested in identical assay conditions, vesicles prepared at pH 8.0 displayed faster and more pronounced dequenching curves and did not respond to activation by c-di-AMP (Fig. 4A-B). Importantly, addition of recombinant KhtT to the external bath of the vesicles reduced the rate of ACMA dequenching from ~0.007 s^{-1} to ~0.002 s^{-1}, at pH 7.5, and ~0.01 s^{-1} to ~0.004 s^{-1}, at pH 8.5, and resulted in recovery of c-di-AMP sensitivity (Fig. 4C). This demonstrated that KhtT was being washed away from KhtU at high pH, giving rise to KhtU-vesicles that did not respond to c-di-AMP, and that it is possible to reassemble the complex by adding the regulatory protein. The binding affinity of KhtT for KhtU at pH 7.5 was estimated from a functional titration of KhtU-vesicles with KhtT, displaying a $K_{1/2}$ ~0.5 µM (SI Appendix, Fig. S5D). The mutant $KhtT_{R110A}$ behaved similarly. It also dissembled from KhtU at high pH, associated and inhibited KhtU activity as efficiently at pH 7.5 and had similar basal activity (SI Appendix, Fig. S5D-E).

We can now compare the functional properties of KhtU alone with those of KhtTU and understand better the mechanisms of activation by c-di-AMP and pH. Strikingly, and although some variation in flux rates was observed between vesicles prepared from different cell culture batches, the experiments above reveal a parallel in the flux activity of KhtTU- and KhtU-vesicles. Flux rates for KhtU increase with pH and in particular, the maximal flux rate measured for KhtTU-vesicles incubated with saturating concentrations of c-di-AMP (see previous section) is identical (~0.01 s^{-1}) to that measured from KhtU-vesicles without KhtT added (Fig. 4C). This leads us to propose that the fully active state of KhtTU is functionally similar to that of KhtU. Based on this, we estimated the maximum flux rate (0.007 s^{-1}) for KhtTU-vesicles with saturating amounts of c-di-AMP at pH 7.5 (which we could not measure due to the large nucleotide concentrations required) from measurements of KhtU-vesicles at the same pH.

We also wondered what happens with cation selectivity in KhtU, another functional property previously described for KhtTU (38). Addition of 10 mM KCl to KhtU-vesicles (at pH 8.5) caused dequenching that is markedly different from no addition or addition of 10 mM choline salt (an organic cation that will not permeate through KhtU). Adding 100 mM KCl intensified dequenching further (Fig. 4D). In contrast, addition of 10 mM NaCl resembles no addition, while addition of 100 mM NaCl or choline chloride results in further quenching of fluorescence, probably due to a change in vesicle volume caused by increased external osmolarity that is not compensated by KhtU-mediated ion influx. We also tested a mixture of 10 mM KCl and 90 mM NaCl. In these conditions, the

fluorescence curve resembles that with 10 mM KCl alone. Experiments at pH 7.5 showed similar results but with less pronounced dequenching curves. Determination of dequenching rates showed that at pH 7.5 there is an increase in ion flux when the K^+ concentration rises from 10 to 100 mM, with rates changing from ~0.003 to ~0.007 s^{-1}. In contrast, at pH 8.5 with 10 mM KCl, flux is already at maximum since there is no change in the dequenching rate with 100 mM KCl, indicating higher affinity of KhtU for K^+ at pH 8.5 (Fig. 4E). Overall, these results demonstrate that except for c-di-AMP sensitivity, KhtU alone displays similar functional properties to KhtTU (38). It is very selective for K^+ over Na^+ and has similar pH dependence, with higher activity at higher pH values.

The falling apart of the KhtTU complex during preparation of everted vesicles at high pH and the similar flux rate measured for KhtU-vesicles and KhtTU-vesicles with saturating concentrations of c-di-AMP raised the possibility that the mechanism of activation by c-d-AMP and pH involves disruption of the interaction between KhtT and KhtU.

To explore this hypothesis, we incubated C-terminal hexahistidine tagged KhtT ($KhtT_{His}$) with KhtU-vesicles at pH 7.0 and isolated the KhtU-vesicles, with associated $KhtT_{His}$, by ultracentrifugation. We incubated these vesicles with 200 µM c-di-AMP or c-di-GMP (negative control), a concentration that is 5-200 fold above $K_{1/2}$ of activation for c-di-AMP, at pH 7.5 or pH 8.0 for 10 minutes. The vesicles were then subjected to a second ultracentrifugation after which free and vesicle-bound $KhtT_{His}$ was detected by western blot, in the supernatant and pellet respectively. In contrast to the c-di-GMP control, c-di-AMP reduced $KhtT_{His}$ associated with the pelleted vesicles and increased the amount of free $KhtT_{His}$ in the supernatant at both pHs tested (Fig. 4F). In parallel, we showed that everted vesicles prepared from cells co-expressing $KhtT_{His}$ and KhtU are still activated by c-di-AMP (SI Appendix, Fig. S9A). The western blot results appear to strongly support the hypothesis that c-di-AMP activation involves detachment of the KhtT:c-di-AMP complex from KhtU. However, comparing the levels of KhtT associated with KhtU-vesicles and vesicles prepared with empty plasmid (empty-vesicles) (SI Appendix, Fig. S9B), after incubation with c-di-AMP, clearly shows that not all KhtT detaches from the vesicles despite the relatively long incubation time and the saturating concentration of nucleotide. Moreover, there is little or no difference between experiments performed at pH 7.5 and 8.0 (Fig. 4F), contrasting with what was observed with the preparation of KhtU-vesicles at high pH. It is therefore more likely that c-di-AMP and pH lead to structural alterations that weaken the KhtT-KhtU interaction, resulting in the activation of KhtU-mediated K^+/H^+ antiport. In experimental situations that include long incubations and repeated washes the complex falls apart, as seen with vesicles prepared at pH 8.0.

In contrast to the function of the C-domain in nucleotide binding, the function of the N-domain is less clear. We wondered if its role is to mediate the interaction with KhtU and to act as a conduit for the conformational change occurring in the C-domain upon binding/unbinding of the nucleotide. Incubation of different KhtT protein variants (full-length KhtT, N-KhtT (corresponding to the N-domain) and C-KhtT (corresponding to C-domain)) with empty-vesicles or KhtU-vesicles followed by ultracentrifugation revealed the levels of protein associated with KhtU (Fig. 4H). A simple quantification was performed by determining the ratio $(I_{KhtU} - I_{empty})/I_{input}$, where I_{KhtU} is the intensity of the signal associated with KhtU-vesicles, I_{empty} corresponds to background signal associated with the empty-vesicles and I_{input} is the signal in the input lanes and accounts for differences is blot transfer efficiency. The ratios were 0.14 and 0.22 for N-KhtT from two independent experiments, and 1.21 and 1.04 for KhtT, indicating that the N-domain forms interactions with KhtU but not as efficiently as full-length KhtT. In contrast, the ratio for C-KhtT is very low, 0.01 from a single experiment where a band was detectable, indicating that C-domain alone is unlikely to bind KhtU. Moreover, unlike full-length KhtT, supplementation of truncated N-domain to KhtU-vesicles up to 10 µM has little or no effect in the dequenching rates at either pH (Fig. 4G).

In addition, in the absence of apo-KhtT crystals we crystallized the truncated N-domain as we reasoned that truncation of the C-domain could release the constraints imposed by the nucleotide-binding domain and reveal a conformational change in the N-domain of KhtT. We solved the structure of the N-domain of KhtT (N-KhtT protein) (up to Gly68) at different pHs (6.5, 7.5 and 8.5) and in different space groups. Besides local changes in the organization of some loops, we do not observe any major alterations in the overall structure relative to the structure of the full-length KhtT. All the structures could be nicely superposed (SI Appendix, Fig. S10), revealing considerable stability and rigidity of the N-domain, independent of pH and crystal packing.

We conclude that the N-domain alone associates weakly with KhtU, does not inhibit KhtU activity and that its structure is not affected by the presence of the C-domain or likely, by binding of c-di-AMP. We propose therefore that the function of the N-domain is to mediate some of the contacts established between KhtT and KhtU, while the C-domain binds c-di-AMP and undergoes a nucleotide-dependent conformational change that weakens the interaction between the KhtT and KhtU, resulting in the activation of the antiporter.

Role of KhtTU in K^+ and pH homeostasis

We have established that KhtTU is regulated by both c-di-AMP and pH. To understand how these modulatory factors fit with the physiological role of KhtTU, we analyzed the impact of this K^+ transporter on growth phenotypes in its native bacterium.

The Δ*khtU* strain (where the *khtU* gene was replaced for an antibiotic cassette in the *B. subtilis* strain 168) was obtained from the Bacillus Genetic Stock Center. It revealed no obvious growth phenotype in a diverse set of growth conditions, with both low and high K^+ concentrations, relative to the wild-type strain (example shown in SI Appendix, Fig. S11A). In contrast, expression of KhtU in the Δ*khtU* strain using the bacitracin-inducible plasmid pBS0E in Spizizen Minimal Medium (SMM) at pH ~7.0 and containing only 2 mM KCl caused a strong growth impairment relative to a strain with the empty vector (Fig. 5A and SI Appendix, Fig. S11B-C). The growth defect was partially complemented by the presence of 100 mM KCl in the growth media (Fig. 5B). Higher concentrations did not improve the outcome (SI Appendix, Fig. S11D). This is consistent with the proposed role of KhtU as a K^+ exporter (37), where unregulated expression results in a toxic effect through a decrease in intracellular K^+. On the other hand, when we co-expressed KhtU and its regulatory subunit KhtT in the Δ*khtU* strain, we saw a recovery in bacterial growth relative to expression of KhtU alone, both at 2 mM and 100 mM K^+ (Fig. 5), indicating that KhtT inhibits the function of KhtU, in accordance with our *in vitro* data and previous findings (37).

I*n vitro* experiments have shown that KhtU transports H^+. Therefore, we analyzed the impact of KhtU and KhtTU expression on pH homeostasis by comparing cell growth in YPD buffered with Bis-tris propane at pH 7.0 and 9.0. The composition of this medium does not include any added monovalent cation. While all strains grew similarly well at pH 7.0, they did not grow at pH 9.0 over a period of 12 h (Fig. 6A-C). In contrast, supplementation of the medium at pH 9.0 with 100 mM KCl allowed cells expressing KhtU to grow after a ~6 h lag period but not the strain with empty plasmid (Fig. 6D). Co-expression of KhtT and KhtU also resulted in cell growth at pH 9.0 with 100 mM KCl but appeared to display a slightly longer lag period. Interestingly, cells co-expressing KhtU and $KhtT_{R110A}$ mutant ($KhtT_{R110A}U$) did not grow, in agreement with the inhibition of KhtU activity by the KhtT mutant that is insensitive to c-di-AMP activation. $KhtT_{R110A}$ expressed as well or slightly better than wild type KhtT as inferred from peptide mass spectrometry analysis of cell extracts from Δ*khtU* strains transformed with empty pBS0E, pBS0E-*KhtTU* and pBS0E-$KhtT_{R110A}U$ (SI Appendix, Fig. S12 and Table S3). Relative KhtT and $KhtT_{R110A}$ abundance was estimated as ~$4.1x10^8$ and ~$7.9x10^8$, respectively, after normalization by total peptide amount. In addition, both protein variants were found among the top 10 most abundant proteins of similar molecular size while the strain with empty plasmid showed much lower levels of native KhtT (position 150 in the abundance ranking).

Importantly, we have also shown above that the mutant $KhtT_{R110A}$ inhibits KhtU as efficiently as the wild type protein (SI Appendix, Fig. S5D) and that at pH 8.0, 8.5 and 9.0 displays slightly higher thermal stability (SI Appendix, Fig. S5B and S5F). Altogether, these results demonstrate that the KhtU antiporter can contribute for bacterial adaptation to alkaline conditions and that c-di-AMP has a role in this process.

Discussion

With this work, we have established that the second messenger c-di-AMP directly affects the function of a K^+ transporter, in this case, as an activator of the K^+ exporter KhtTU. We have quantified this effect, defined the molecular details of the interaction between c-di-AMP and the cytosolic protein KhtT and validated the role of KhtTU, and of its membrane protein component KhtU, in a physiological context. Overall, these data provide strong support to the proposal that c-di-AMP has a central role in the regulation of the K^+ homeostasis machinery in *B. subtilis* and in other bacterial species, including pathogens.

Importantly, our data revealed that KhtTU activation by c-di-AMP is highly dependent on pH. A pH increase from 7.5 to 8.5 shifts the $K_{1/2}$ of c-di-AMP activation by ~60-fold, from ~40 μM at pH 7.5 to less than 1 μM at pH 8.5. This shows that to understand the role of c-di-AMP in the modulation of the bacterial intracellular K^+ concentration, we need to consider what other factors regulate the function of the K^+ transporters in the cell and how these factors affect c-di-AMP regulation.

We have also gained good insights into the mechanism of activation of KhtTU by c-di-AMP and pH. In particular, we have found that KhtT is responsible for tight binding of the nucleotide and that, in contrast, KhtU is c-di-AMP insensitive but is activated by high pH, with its flux rate increasing from 0.007 s^{-1} at pH 7.5 to 0.1 s^{-1} at pH 8.5. Strikingly, this pH-dependence is mirrored in the KhtTU complex, where the basal (in the absence of c-di-AMP) and maximal (with saturating concentrations of c-di-AMP) flux rates also increase when pH changes from 7.5 to 8.5. The pH dependence shown by KhtU, including the apparent increase in the affinity for K^+ at high pH, closely resemble the properties of other proteins from the Cation-Proton-Antiporter (CPA) superfamily such as the well-studied Na^+/H^+ antiporter NhaA from *E. coli*, which lacks a cytosolic subunit (42, 43). Our results also suggest that c-di-AMP binding weakens the KhtT-KhtU interaction. Therefore, we propose a model where KhtU functions as a "typical" cation/H^+ antiporter of the CPA superfamily and apo-KhtT acts as a "loose brake" that slows the transport cycle of the antiporter but does not impede it, so that in KhtTU we observe basal pH-dependent flux even in the absence of c-di-AMP. Upon c-di-

AMP binding there is a conformational change in the C-domain of KhtT that weakens the interaction with KhtU, allowing the membrane protein to undergo its transport cycle at maximum rate. Interestingly, this mechanism resembles that proposed for c-di-AMP regulation of the Trk channel SPD_0076 from Streptococcus pneumonia (44). Binding of c-di-AMP to the RCK regulatory protein, CapB, results in the disassembly of the functional complex formed by SPD_076 and CapB and inactivation of K^+ uptake.

Strikingly, our data showed that expression of KhtU and KhtTU (independently of the original promoter) in the native bacterium B. subtilis affects growth in a K^+- and pH-dependent way, providing a physiological context for the regulation of KhtTU activity. In particular, expression of KhtU and KhtTU prove to be fundamental for bacterial growth at pH 9.0 when K^+ is available in the media. It is not straightforward to understand this gain-of-function phenotype since addition of K^+ to the external medium should decrease the K^+ gradient that drives H^+ uptake in a K^+/H^+ antiporter. Nevertheless, these results demonstrate that KhtTU can contribute to alkaline adaptation. This gain of function at high pH allowed us to demonstrate that c-di-AMP has a role in the regulation of KhtTU in a physiological context since co-expression of KhtU with a KhtT mutant that is insensitive to c-di-AMP ($KhtT_{R110A}$) generated a strain that did not adapt to alkaline conditions.

It has been determined that the average concentration of c-di-AMP in *B. subtilis* varies between 1-5 μM (45) and shown that c-di-AMP concentration rises as intracellular K^+ increases (17, 26). Therefore, the high activation $K_{1/2}$ determined for KhtTU (~40 μM) at a "normal" intracellular pH (pH ~7.5) fits nicely with the idea that with rising concentrations of K^+ and consequently, rising c-di-AMP, KhtTU becomes more active and transports K^+ out of the cell. Reduction in intracellular K^+ concentration, is reflected in lower c-di-AMP availability, reducing KhtTU activity back to basal levels. In addition, when intracellular pH becomes too high, both basal and maximal activity of KhtTU, and its sensitivity to c-di-AMP increase ($K_{1/2} < 1$ μM), requiring lower amounts of c-di-AMP to fully activate KhtTU. These properties, transform KhtTU into a H^+ importer in alkaline conditions, providing support for a role of KhtTU in pH homeostasis. It is worthwhile pointing out that our *in vivo* results with the $KhtT_{R110A}$ mutant indicate that in alkaline conditions c-di-AMP signaling is still important for the activity of KhtTU, suggesting that besides its role as a master regulator of K^+ homeostasis, c-di-AMP also has a role in pH homeostasis.

Materials and Methods

Extended Materials and Methods are described in Supplementary Information.

Expression and purification of KhtT protein variants

Full-length KhtT, $KhtT_{His}$, $KhtT_{R110A}$, N-KhtT, N_{His}-KhtT and C_{His}-KhtT were expressed in *Escherichia coli* BL21 (DE3) or B834 (DE3) (for production of selenomethionine substituted protein) after induction with IPTG at 37°C. Proteins were purified by affinity chromatography in Ni^{2+}-beads and size-exclusion chromatography.

Isothermal titration calorimetry and Thermal shift assay

Recombinant KhtT and $KhtT_{R110A}$ were titrated with c-di-AMP (or c-di-GMP for KhtT) in a MicroCal VP-ITC instrument (GE Healthcare). Data were visualized and analyzed with Origin 7 Software using a single binding site model. Melting temperatures of KhtT and $KhtT_{R110A}$, in presence and in absence of c-di-AMP or c-di-GMP were determined by Sypro Orange thermal shift assay.

Structure determination

Diffraction data were collected at beamlines XALOC of ALBA and PROXIMA-1 of SOLEIL. X-ray diffraction data collection and processing statistics are summarized in SI Appendix, Table S1. The high-resolution structure of KhtT:c-di-AMP complex was solved by SAD, using the anomalous signal of selenium and NCS-averaging. The low-resolution KhtT and its N-domain structures were solved by molecular replacement. Refinement statistics are summarized in Table S1. Refined coordinates and structure factors were deposited at the Protein Data Bank (46): 7AGV – high-resolution KhtT structure; 7AHM – low-resolution KhtT structure; 7AGW – N-domain of KhtT at pH 6.5; 7AHT – N-domain of KhtT at pH 7.5; 7AGY – N-domain of KhtT at pH 8.5.

Preparation of everted membrane vesicles

Everted membrane vesicles were prepared as previously described (47) from KNabc *E. coli* strain transformed with pQE60-*khtTU* (for KhtTU- or KhtU-vesicles), pQE60-$khtT_{His}U$, pQE60-$khtT_{R110A}U$ or pQE60 (for empty vesicles) at pH 7.0 (for preparation of KhtTU-, $KhtT_{R110A}$U-, $KhtT_{His}$U- or empty-vesicles) or pH 8.0 (for preparation of KhtU-vesicles).

Antiport Assays

Fluorescence-based flux assays were performed at room temperature in a FluoroMax-4 spectrofluorometer (Horiba) with excitation at 410 nm and emission at 480 nm. Everted vesicles were

mixed with 2 µM 9-amino-6-chloro-2-methoxyacridine (ACMA). Assays were initiated with addition of 4 mM sodium lactate to promote a respiration-generated ΔpH followed by 50 mM KCl (unless otherwise noted) in different conditions.

KhtT interaction with KhtU

Everted membrane vesicles produced were incubated with KhtT, N-KhtT or C-KhtT with C-terminal hexahistidine tags, followed by ultra-centrifugations and analysis of supernatant and pellets by Western blot using an anti-His antibody and HRP-conjugated secondary antibody. Detection was done using ECL Prime Western Blotting System (GE Healthcare).

***B. subtilis* culture conditions**

For K^+ homeostasis experiments, *B. subtilis* strain Δ*khtU* transformed with pBS0E, pBS0E-*khtU*, pBS0E-*khtTU* or pBS0E-*khtT*$_{R110A}$*U* were grown in SMM supplemented with antibiotics and bacitracin (protein expression inducer). All growth medium conditions included 150 mM of monovalent cations (mixture of Na^+ and K^+) and pH was ~7.0. For experiments at different pH, strains were grown in YPD medium, buffered at pH 7.0 or pH 9.0 with and without 100 mM KCl and supplemented with antibiotics and bacitracin. Expression levels of KhtT and KhtT$_{R110A}$ in Δ*khtU* with pBS0E, pBS0E-*khtTU* or pBS0E-*khtT*$_{R110A}$*U* were estimated by peptide mass spectrometry of cell extracts from cultures grown in YPD medium at pH 7.0, since the Δ*khtU* (pBS0E-*khtT*$_{R110A}$*U*) strain does not grow at pH 9.0.

Acknowledgments

We acknowledge the SOLEIL and ALBA synchrotrons for access and thank their staff for help with data collection. Support of the Biochemical and Biophysical Technologies, Cell Culture and Genotyping and X-ray Crystallography scientific platforms of i3S (Porto, Portugal) is also acknowledged. Mass spectrometry analysis was performed by Hugo Osório at the i3S Proteomics Scientific Platform. This work had support from the Portuguese Mass Spectrometry Network, integrated in the National Roadmap of Research Infrastructures of Strategic Relevance (ROTEIRO/0028/2013; LISBOA-01-0145-FEDER-022125). Work was supported by FEDER - Fundo Europeu de Desenvolvimento Regional funds through the COMPETE 2020-Operational Programme for Competitiveness and Internationalization (POCI), Portugal 2020, and by Portuguese funds through FCT - Fundação para a Ciência e a Tecnologia/Ministério da Ciência, Tecnologia e Ensino Superior in the framework of the projects POCI-01–0145-FEDER-029863(PTDC/BIA-BQM/29863/2017) and by Fundação Luso-Americana para o Desenvolvimento through the FLAD Life Science 2020 award 'Bacterial K^+ transporters are potential antimicrobial targets: mechanisms of transport and regulation'.

Author´s contributions

Conception and design of study: TBC and JHM-C; Data collection and analysis: TBC, JPLG, JMPJ and JHM-C; Drafting of manuscript: TBC and JHM-C. Critical revision of manuscript: TBC, JPLG, JMPJ and JHM-C.

Declaration of interests

The authors declare no competing interests.

References

1. Zaver SA & Woodward JJ Cyclic dinucleotides at the forefront of innate immunity. *Curr Opin Cell Biol* **63**, 49-56 (2020).
2. Krasteva PV & Sondermann H Versatile modes of cellular regulation via cyclic dinucleotides. *Nat Chem Biol* **13**, 350-359 (2017).
3. Aline Dias da P, Nathalia Marins de A, Gabriel Guarany de A, Robson Francisco de S, & Cristiane Rodrigues G The World of Cyclic Dinucleotides in Bacterial Behavior. *Molecules* **25,** 2462 (2020).
4. Commichau FM, Heidemann JL, Ficner R, & Stulke J Making and Breaking of an Essential Poison: the Cyclases and Phosphodiesterases That Produce and Degrade the Essential Second Messenger Cyclic di-AMP in Bacteria. *J Bacteriol* **201,** e00462-00418 (2019).
5. Huynh TN & Woodward JJ Too much of a good thing: regulated depletion of c-di-AMP in the bacterial cytoplasm. *Curr Opin Microbiol* **30**, 22-29 (2016).
6. Fahmi T, Port GC, & Cho KH c-di-AMP: An Essential Molecule in the Signaling Pathways that Regulate the Viability and Virulence of Gram-Positive Bacteria. *Genes (Basel)* **8**, 197 (2017).
7. Commichau FM, Dickmanns A, Gundlach J, Ficner R, & Stulke J A jack of all trades: the multiple roles of the unique essential second messenger cyclic di-AMP. *Mol Microbiol* **97,** 189-204 (2015).
8. Stulke J & Kruger L Cyclic di-AMP Signaling in Bacteria. *Annu Rev Microbiol* **74**, 159-179 (2020).
9. Sureka K, *et al.* The cyclic dinucleotide c-di-AMP is an allosteric regulator of metabolic enzyme function. *Cell* **158**, 1389-1401 (2014).
10. Luo Y & Helmann JD Analysis of the role of Bacillus subtilis sigma(M) in beta-lactam resistance reveals an essential role for c-di-AMP in peptidoglycan homeostasis. *Mol Microbiol* **83**, 623-639 (2012).
11. Corrigan RM, Abbott JC, Burhenne H, Kaever V, & Grundling A c-di-AMP is a new second messenger in Staphylococcus aureus with a role in controlling cell size and envelope stress. *PLoS Pathog* **7**, e1002217 (2011).
12. Peng X, Zhang Y, Bai G, Zhou X, & Wu H Cyclic di-AMP mediates biofilm formation. *Mol Microbiol* **99**, 945-959 (2016).
13. Gundlach J, Rath H, Herzberg C, Mader U, & Stulke J Second Messenger Signaling in Bacillus subtilis: Accumulation of Cyclic di-AMP Inhibits Biofilm Formation. *Front Microbiol* **7**, 804 (2016).
14. Bejerano-Sagie M, *et al.* A checkpoint protein that scans the chromosome for damage at the start of sporulation in Bacillus subtilis. *Cell* **125**, 679-690 (2006).
15. Cho KH & Kang SO Streptococcus pyogenes c-di-AMP phosphodiesterase, GdpP, influences SpeB processing and virulence. *PLoS One* **8**, e69425 (2013).
16. Gundlach J, Commichau FM, & Stulke J Perspective of ions and messengers: an intricate link between potassium, glutamate, and cyclic di-AMP. *Curr Genet* **64**, 191-195 (2018).
17. Gundlach J, *et al.* Control of potassium homeostasis is an essential function of the second messenger cyclic di-AMP in Bacillus subtilis. *Sci Signal* **10**, eaal3011 (2017).
18. Gundlach J, *et al.* Adaptation of Bacillus subtilis to Life at Extreme Potassium Limitation. *mBio* **8**, e00861-00817 (2017).
19. Zarrella TM, Metzger DW, & Bai G Stress Suppressor Screening Leads to Detection of Regulation of Cyclic di-AMP Homeostasis by a Trk Family Effector Protein in Streptococcus pneumoniae. *J Bacteriol* **200,** e00045-00018 (2018).
20. Rozov A, *et al.* Importance of potassium ions for ribosome structure and function revealed by long-wavelength X-ray diffraction. *Nat Commun* **10**, 2519 (2019).
21. Bakker EP & Mangerich WE Interconversion of components of the bacterial proton motive force by electrogenic potassium transport. *J Bacteriol* **147**, 820-826 (1981).
22. Kroll RG & Booth IR The role of potassium transport in the generation of a pH gradient in Escherichia coli. *Biochem J* **198**, 691-698 (1981).
23. Meury J, Robin A, & Monnier-Champeix P Turgor-controlled K+ fluxes and their pathways in Escherichia coli. *Eur J Biochem* **151**, 613-619 (1985).
24. Epstein W & Schultz SG Cation Transport in Escherichia coli: V. Regulation of cation content. *J Gen Physiol* **49**, 221-234 (1965).
25. Whatmore AM, Chudek JA, & Reed RH The effects of osmotic upshock on the intracellular solute pools of Bacillus subtilis. *J Gen Microbiol* **136**, 2527-2535 (1990).

26. Pham HT, *et al.* Enhanced uptake of potassium or glycine betaine or export of cyclic-di-AMP restores osmoresistance in a high cyclic-di-AMP Lactococcus lactis mutant. *PLoS Genet* **14**, e1007574 (2018).
27. Devaux L, *et al.* Cyclic di-AMP regulation of osmotic homeostasis is essential in Group B Streptococcus. *PLoS Genet* **14**, e1007342 (2018).
28. Zeden MS, *et al.* Cyclic di-adenosine monophosphate (c-di-AMP) is required for osmotic regulation in Staphylococcus aureus but dispensable for viability in anaerobic conditions. *J Biol Chem* **293**, 3180-3200 (2018).
29. Quintana IM, *et al.* The KupA and KupB Proteins of Lactococcus lactis IL1403 Are Novel c-di-AMP Receptor Proteins Responsible for Potassium Uptake. *J Bacteriol* **201**, e00028-00019 (2019).
30. Gundlach J, *et al.* Sustained sensing in potassium homeostasis: Cyclic di-AMP controls potassium uptake by KimA at the levels of expression and activity. *J Biol Chem* **294**, 9605-9614 (2019).
31. Nelson JW, *et al.* Riboswitches in eubacteria sense the second messenger c-di-AMP. *Nat Chem Biol* **9**, 834-839 (2013).
32. Chin KH, *et al.* Structural Insights into the Distinct Binding Mode of Cyclic Di-AMP with SaCpaA_RCK. *Biochemistry* **54**, 4936-4951 (2015).
33. Rocha R, Teixeira-Duarte CM, Jorge JMP, & Morais-Cabral JH Characterization of the molecular properties of KtrC, a second RCK domain that regulates a Ktr channel in Bacillus subtilis. *J Struct Biol* **205**, 34-43 (2019).
34. Kim H, *et al.* Structural Studies of Potassium Transport Protein KtrA Regulator of Conductance of K+ (RCK) C Domain in Complex with Cyclic Diadenosine Monophosphate (c-di-AMP). *J Biol Chem* **290**, 16393-16402 (2015).
35. Corrigan RM, *et al.* Systematic identification of conserved bacterial c-di-AMP receptor proteins. *Proc Natl Acad Sci U S A* **110**, 9084-9089 (2013).
36. Moscoso JA, *et al.* Binding of Cyclic Di-AMP to the Staphylococcus aureus Sensor Kinase KdpD Occurs via the Universal Stress Protein Domain and Downregulates the Expression of the Kdp Potassium Transporter. *J Bacteriol* **198**, 98-110 (2016).
37. Fujisawa M, Wada Y, & Ito M Modulation of the K+ efflux activity of Bacillus subtilis YhaU by YhaT and the C-terminal region of YhaS. *FEMS Microbiol Lett* **231**, 211-217 (2004).
38. Fujisawa M, Ito M, & Krulwich TA Three two-component transporters with channel-like properties have monovalent cation/proton antiport activity. *Proc Natl Acad Sci U S A* **104**, 13289-13294 (2007).
39. Guo Q, *et al.* Using a phenotype microarray and transcriptome analysis to elucidate multi-drug resistance regulated by the PhoR/PhoP two-component system in Bacillus subtilis strain NCD-2. *Microbiol Res* **239**, 126557 (2020).
40. Chandrangsu P, Dusi R, Hamilton CJ, & Helmann JD Methylglyoxal resistance in Bacillus subtilis: contributions of bacillithiol-dependent and independent pathways. *Mol Microbiol* **91**, 706-715 (2014).
41. Rosen BP Ion extrusion systems in Escherichia coli. *Methods Enzymol* **125**, 328-336 (1986).
42. Taglicht D, Padan E, & Schuldiner S Overproduction and purification of a functional Na+/H+ antiporter coded by nhaA (ant) from Escherichia coli. *J Biol Chem* **266**, 11289-11294 (1991).
43. Padan E Functional and structural dynamics of NhaA, a prototype for Na(+) and H(+) antiporters, which are responsible for Na(+) and H(+) homeostasis in cells. *Biochim Biophys Acta* **1837**, 1047-1062 (2014).
44. Bai Y, *et al.* Cyclic di-AMP impairs potassium uptake mediated by a cyclic di-AMP binding protein in Streptococcus pneumoniae. *J Bacteriol* **196**, 614-623 (2014).
45. Oppenheimer-Shaanan Y, Wexselblatt E, Katzhendler J, Yavin E, & Ben-Yehuda S c-di-AMP reports DNA integrity during sporulation in Bacillus subtilis. *EMBO Rep* **12**, 594-601 (2011).
46. Berman HM, *et al.* The Protein Data Bank. *Nucleic Acids Res* **28**, 235-242 (2000).
47. Rosen BP & Tsuchiya T Preparation of everted membrane vesicles from Escherichia coli for the measurement of calcium transport. *Methods Enzymol* **56**, 233-241 (1979).

Figures

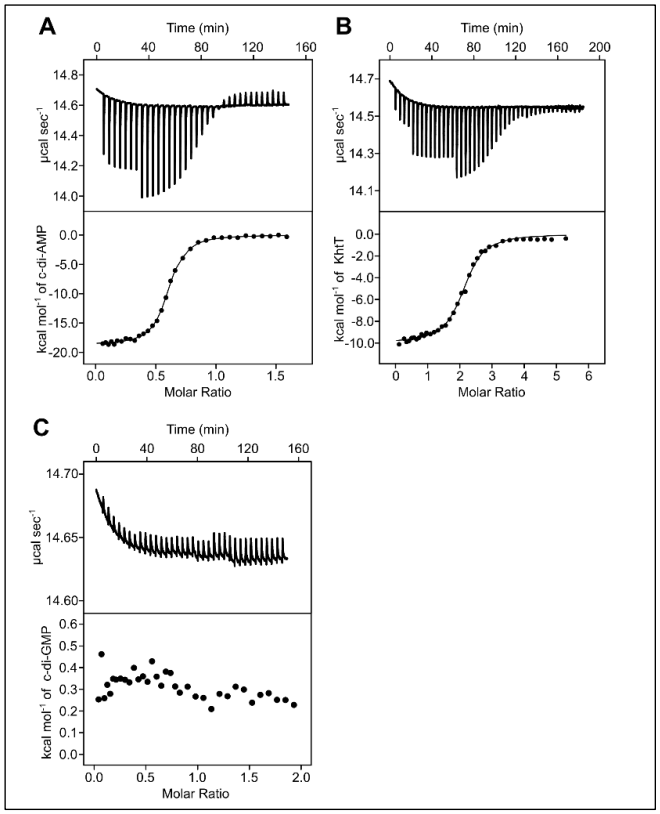

Fig. 1. Characterization of the interaction of c-di-AMP with KhtT using ITC. (A) Titration of c-di-AMP (152 µM) into KhtT (18 µM). (B) Titration of KhtT (175 µM) into c-di-AMP (6 µM). (C) Titration of c-di-GMP (308 µM) into KhtT (35 µM). Top panels show the raw titration heat values plotted as a function of time and bottom panels show normalized integration heat values of injectant plotted as a function of molar ratio. Experiments were performed at pH 8.0 and 25°C. Curves shown in bottom panels corresponds to a single binding site model. See also SI Appendix, Fig. S8.

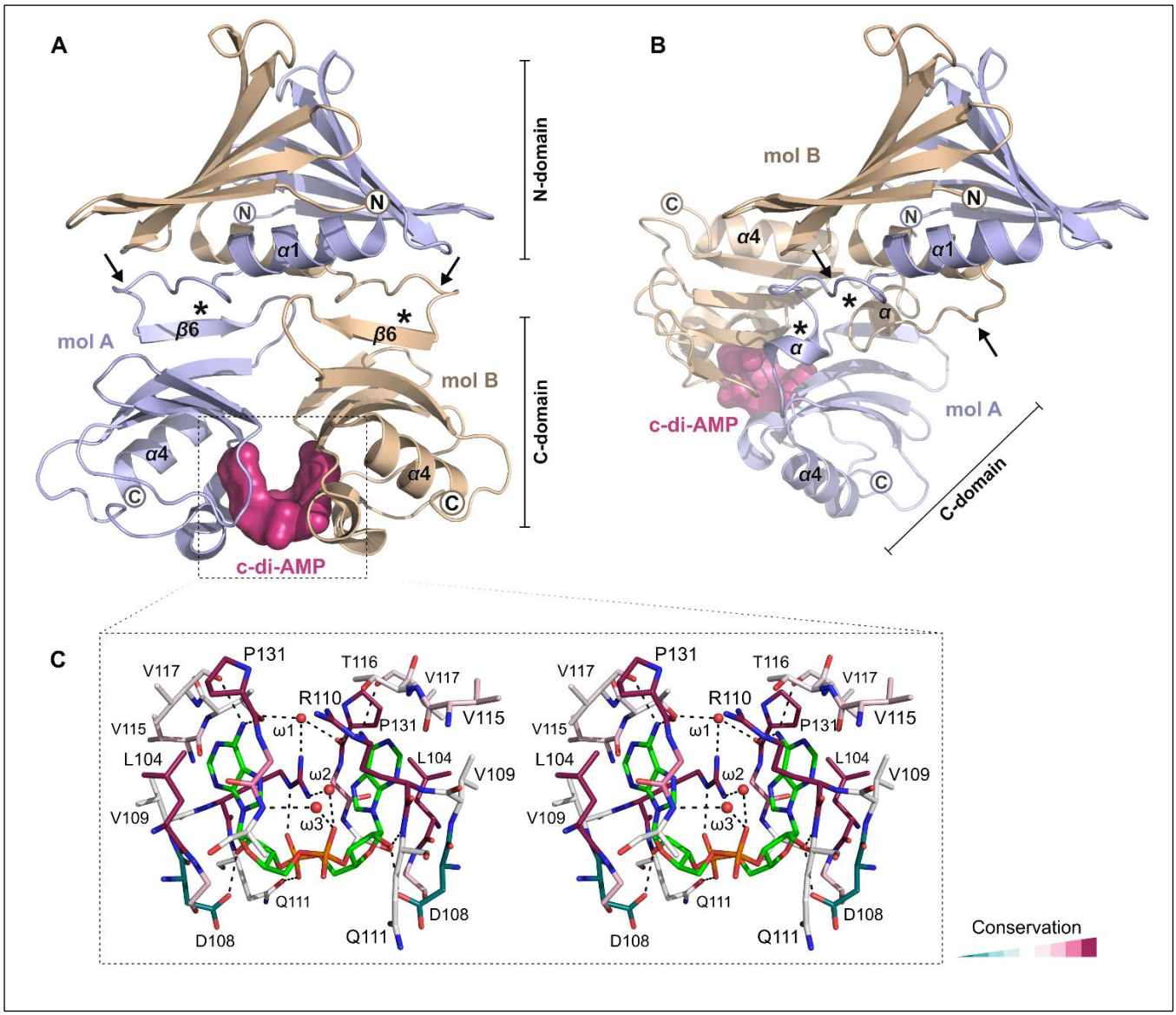

Fig. 2. Crystal structure of KhtT with bound c-di-AMP. (A) Cartoon representation of three-dimensional structure of KhtT in complex with c-di-AMP obtained from high-resolution monoclinic crystal. Monomers are colored in blue (molecule A) and wheat (molecule B). N- and C-domains are indicated. Surface representation of c-di-AMP is colored pink. Linkers connecting N- and C-domains are indicated by arrows. Secondary structure elements that differ in the crystallographic structure shown in A and B are indicated by an asterisk. (B) Cartoon representation of the low-resolution structure of KhtT:c-di-AMP complex obtained from tetragonal crystals. All elements are shown as in A. N-domain is in the same orientation as in A. (C) Stereo-view of the c-di-AMP binding site. Residues around c-di-AMP are represented as sticks and colored according to their evolutionary conservation (shown at bottom right of the image), calculated from a multiple sequence alignment of 200 unique amino acid sequences with 95-40% of identity. Water molecules (ω) participating in ligand binding are represented as red spheres. Hydrogen-bonding is indicated by black dashed lines. See also SI Appendix, Fig. S1-S4 and Table S1.

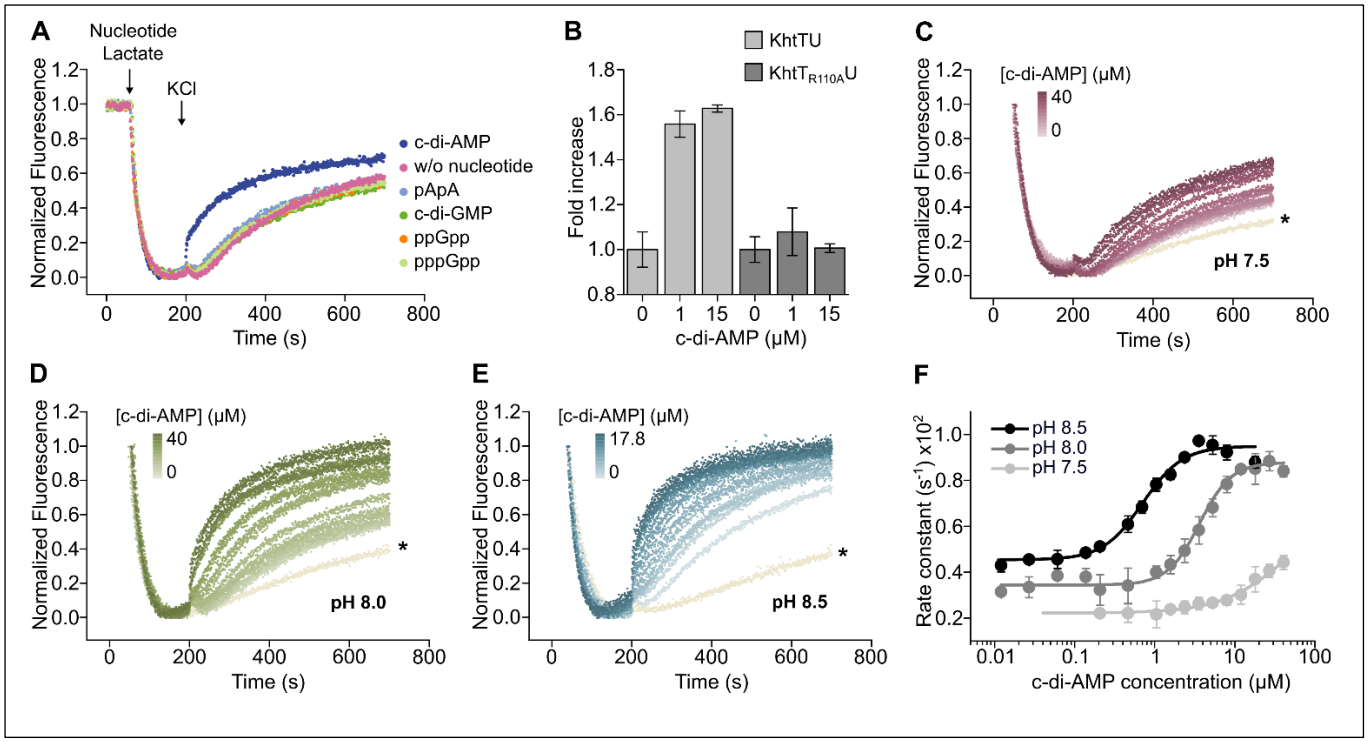

Fig. 3. KhtT is activated by c-di-AMP. (A) Representative fluorescence traces of lactate-dependent quenching and salt-induced (50 mM KCl) dequenching of ACMA for KhtTU-vesicles with (15 μM) and without nucleotides, at pH 8.5. (B) Fold change in rate constant determined from fitting single exponentials to dequenching curves for wild-type KhtTU and mutant $KhtT_{R110A}U$. Mean ± SD are shown for 3-4 experiments performed at pH 8.5 and with 50 mM KCl. (C-E) Normalized fluorescence curves for KhtTU-vesicles with increasing c-di-AMP concentrations (shown by color intensity) in the presence of 50 mM KCl at pH 7.5 (C), 8.0 (D) and 8.5 (E). Leak activity, in the absence of KCl and c-di-AMP, is shown by dequenching curve marked by asterisk. (F) Plot of rate constants *versus* c-di-AMP concentration determined from titrations at different pHs. Mean ± SD are shown for at least 4 independent experiments from two everted-vesicle preparations, excepting the 3 lowest c-di-AMP concentrations at pH 8.0, for which 3 measurements were performed using a single batch of vesicles. Data were fitted with a Hill equation and Hill coefficient (*n*) determined from the fits are $K_{1/2}$ = 0.70 ± 0.08 μM and *n* = 1.76 ± 0.24 (pH 8.5), $K_{1/2}$ = 3.58 ± 0.49 μM and *n* = 2.18 ± 0.44 (pH 8.0), and $K_{1/2}$ = 43.4 ± 2.7 μM and *n* = 1.1 ± 0.1 (pH 7.5). See also SI Appendix, Fig. S5-S7.

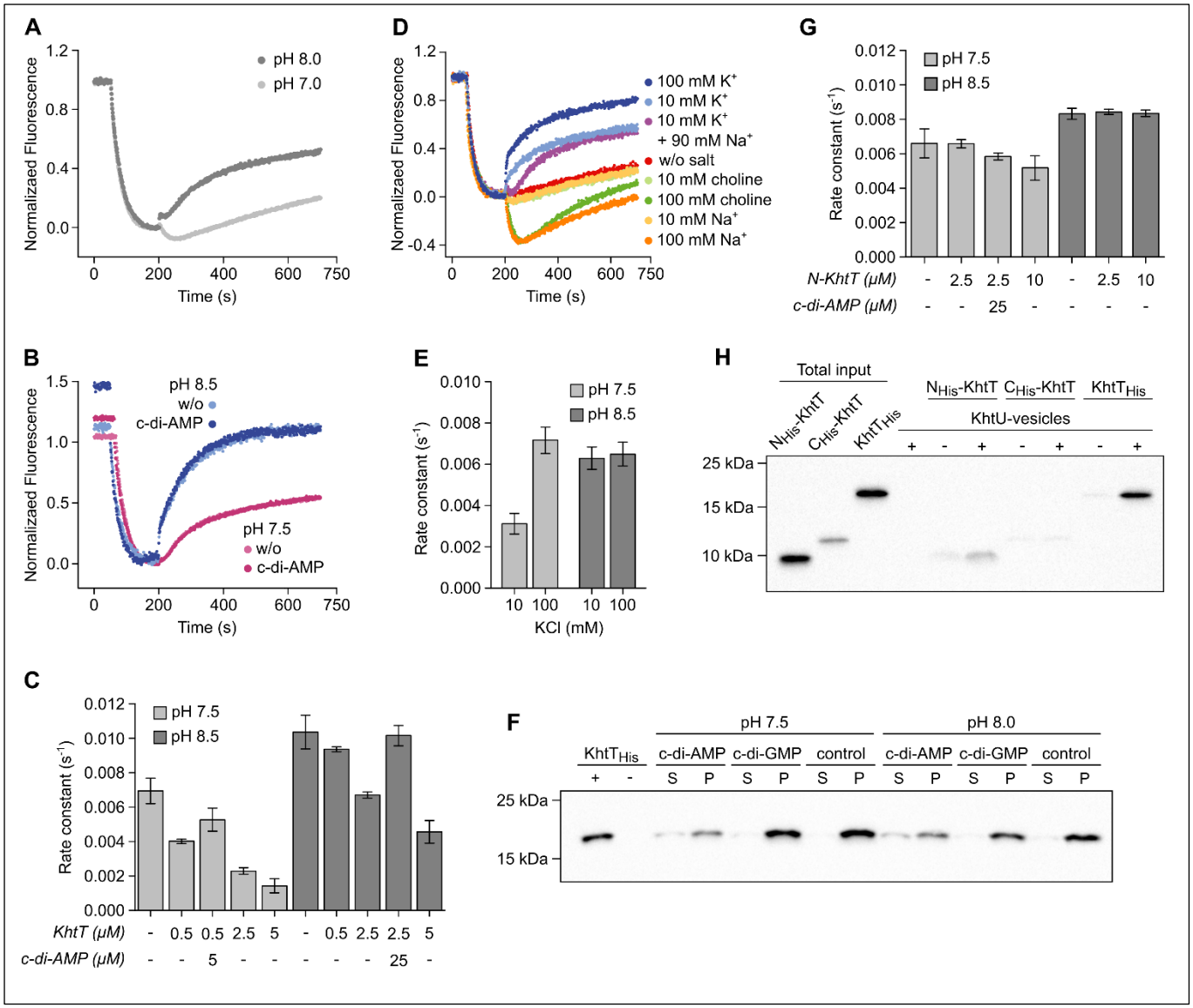

Fig. 4. KhtT-KhtU interaction. (A) Representative fluorescence traces for vesicles prepared at pH 7.0 (light gray) or pH 8.0 (dark gray) and assayed under the same experimental conditions, at pH 7.5. (B) Representative fluorescence traces for vesicles prepared at pH 8.0 and assayed at pH 7.5 (pink) and pH 8.5 (blue) in the presence (dark pink/blue) or absence (light pink/blue) of 25 μM c-di-AMP. (C) Plot of the rate constants measured from dequenching traces of KhtU-vesicles incubated with increasing concentrations of full-length KhtT at pH 7.5 (light gray) and 8.5 (dark gray) with 50 mM KCl, with and without c-di-AMP. (D) Representative fluorescence traces for KhtU-vesicles assayed at pH 8.5 and with added KCl, NaCl, choline chloride or salt mixtures. (E) Plot of rate constants measured from dequenching traces of KhtU-vesicles incubated with 10 or 100 mM KCl at pH 7.5 (light gray) or 8.5 (dark gray). (F) Western blot of supernatant (S) and pellet (P) fractions from ultracentrifugation of KhtU-vesicles+$KhtT_{His}$ after incubation with c-di-AMP, c-di-GMP or assay buffer (control) at pH 7.5 and pH 8.0. Blot was probed with α anti-His. (G) Plot of rate constants measured from dequenching traces of KhtU-vesicles incubated with increasing concentrations of KhtT N-domain at pH 7.5 (light gray) and 8.5 (dark gray). Mean ± SD of 3-4 experiments shown in (C), (E) and (G). (H) Western blot of the pellet fractions from ultracentrifugation of empty or KhtU-vesicles after incubation with N- or C-domain of KhtT (N_{His}-KhtT and C_{His}-KhtT, respectively) or full-length $KhtT_{His}$. Total inputs (mixture of KhtU-containing vesicles with the KhtT variants) were loaded as positive controls. Total input of $KhtT_{His}$ is 3-fold diluted compared to the other inputs, and pellet fractions containing $KhtT_{His}$ are 6-fold diluted compared to the other pellet samples. KhtU-vesicles alone were loaded as negative control. Transfer efficiency into PVDF membrane of KhtT variants varied. See also SI Appendix, Fig. S9-S10.

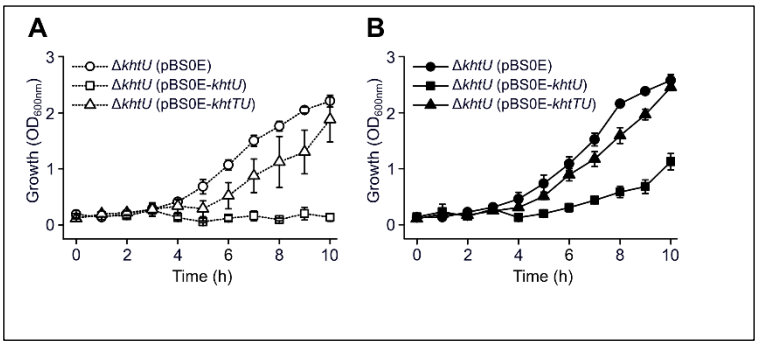

Fig. 5. Impact of KhtU and KhtTU in the growth of *B. subtilis*. Optical density of cell cultures with strains Δ*khtU* (pBS0E), Δ*khtU* (pBS0E-*khtU*) and Δ*khtU* (pBS0E-*khtTU*) growing in SMM, pH ~7.0, with 2 mM (A) or 100 mM (B) KCl. Plots show mean ± SD of triplicate growths from a single experiment. Similar results were obtained with experiments performed in different days. The empty plasmid control strain [Δ*khtU* (pBS0E)] was tested with 100 mM KCl in a single experiment. See also SI Appendix, Fig. S11.

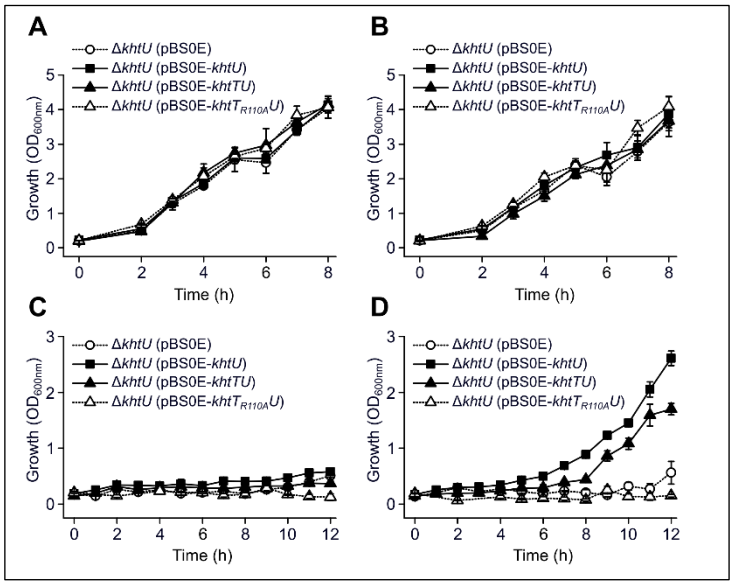

Fig. 6. Impact of the expression of KhtTU in the growth of *B. subtilis* at pH 7.0 and 9.0. Optical density of cell cultures with strains Δ*khtU* (pBS0E), Δ*khtU* (pBS0E-*khtU*), Δ*khtU* (pBS0E-*khtTU*) and Δ*khtU* (pBS0E-*khtT*$_{R110A}$*U*) growing in YPD at pH 7.0 (A and B) or pH 9.0 (C and D) without salt supplementation (A and C) or with 100 mM KCl added (B and D). Plots show mean ± SD of triplicate growths from a single experiment. Similar results were obtained with experiments performed in different days. See also SI Appendix, Fig. S12 and Table S3.